Progress in Oceanography 215 (2023) 103054

Contents lists available at ScienceDirect

Progress in Oceanography

journal homepage: www.elsevier.com/locate/pocean

The summer bacterial and archaeal community composition of the northern Barents Sea

Stefan Thiele [a,b,*], Anna Vader [c], Stuart Thomson [c], Karoline Saubrekka [d], Elzbieta Petelenz [a], Hilde Rief Armo [a], Oliver Müller [a], Lasse Olsen [a], Gunnar Bratbak [a], Lise Øvreås [a,c]

[a] Department of Biological Science, University of Bergen, Thormøhlensgate 53 A/B, 5020 Bergen, Norway
[b] Bjerknes Centre for Climate Research, Jahnebakken 5, 5007 Bergen, Norway
[c] University Center in Svalbard (UNIS), 9171 Longyearbyen, Norway
[d] Department of Bioscience, University of Oslo, Blindernvn. 31, 0371 Oslo, Norway

ARTICLE INFO

Keywords:
Phytoplankton derived carbon
Microbial ecology
Arctic microbes
Nansen Legacy
Bacterial succession
Microbial loop

ABSTRACT

Climate change related alterations in the Arctic have influences on the marine ecosystems, in particular on phytoplankton bloom dynamics. Since phytoplankton blooms are the main provider of carbon sources to the microbial loop, the bacterial and archaeal community are affected by the changes as well. Warmer water and less sea ice can lead to an earlier onset of phytoplankton blooms and consequently also to changes in the bacterial and archaeal community dynamics throughout Arctic summers. Here, we compared the bacterial and archaeal community composition during three summers (2018, 2019, and 2021) along a transect from the Barents Sea to the Arctic Ocean north of Svalbard. We used 16S rRNA gene sequencing to investigate changes in the communities in time and space. The main results showed that, *Gammaproteobacteria* (*Nitrincolaceae*), *Bacteroidia* (*Polaribacter*), and *Alphaproteobacteria* (SAR11 clade 1a members) dominated the bacterial and archaeal community in the surface waters but varied in abundance patterns between the years. The variations are potentially a result of different phytoplankton bloom stages and consequently differences in the availability of carbon sources. The distinctly different deep water communities were dominated by *Candidatus* Nitrosopumilus, *Marinimicrobia*, and members of the SAR324 clade in all years. The results indicate that changes in phytoplankton bloom dynamics can influence bacterial and archaeal community and thereby marine carbon cycling in surface waters, although direct links to the effects of global warming remain uncertain.

1. Introduction

The Arctic warms four times faster than the global average in response to global warming (Rantanen et al., 2022). One of the transition zones between the Atlantic and the Arctic Ocean is the Barents Sea. Here, warm Atlantic water mixes with cold Artic water over a shallow shelf area. The increased warm water import from the Atlantic, a process termed "Atlantification", has lead to 50% decreased sea-ice coverage of the northern Barents Sea within 10 years from 1998 to 2008 (Årthun et al., 2012; Polyakov et al., 2017). These alterations of the Arctic environment may have profound effects on the highly dynamic and sensitive marine ecosystems (Loeng, 1991; Reigstad et al., 2002; Smedsrud et al., 2013; Wassmann et al., 2011). Seasonal investigations of the biological components of the ecosystem are rare which impedes the prediction of the consequences of global warming. The goal of the Nansen Legacy project is to investigate the ecosystem of the Barents Sea and provide a baseline for comparative future studies and ecosystem predictions.Table 1

The first indications for major changes in the Arctic have already been shown, as early phytoplankton blooms were detected under the sea ice and the chances for the occurrence of autumn blooms have increased by 70% (Ardyna et al., 2014; Assmy et al., 2017). This is likely correlated with a prolongation of the vegetative season by 10–15 days due to loss of sea ice cover (Arrigo and van Dijken, 2015). The longer vegetative season may influence various levels of the marine food web, such as fish, copepods, phytoplankton, and also the bacterial and archaeal communities (Haug et al., 2017; Li et al., 2009; Mueter et al., 2009). However, the responses of organisms and food webs, particularly the bacterial and archaeal communities, to changes in environmental factors remain poorly known.

* Corresponding author at: Department of Biological Science, University of Bergen, Thormøhlensgate 53 A/B, 5020 Bergen, Norway.
E-mail address: Stefan.thiele@uib.no (S. Thiele).

https://doi.org/10.1016/j.pocean.2023.103054

Available online 30 May 2023

Most of the marine primary production (>50%) takes place during these phytoplankton spring bloom (Sakshaug, 2004). Such spring blooms are the main source of carbon for many trophic levels in marine ecosystems, including the bacterial and archaeal communities. In the North Sea, the phytoplankton spring bloom are followed by successions of mostly heterotrophic bacteria such as *Bacteroidetes*, *Gammaproteobacteria* and *Roseobacter*, based on the predominant carbon sources (Teeling et al., 2016, 2012). Similar bacterial successions have been found in the polar regions, where a marine community dominated by members of the SAR11 clade (Schattenhofer et al., 2009; Thiele et al., 2012), transfered to a communitywith high relative abundances of *Gammaproteobacteria* (*Oceanospirillaceae*, *Halomonadaceae* and *Alteromonadaceae*), *Bacteroidetes* (*Polaribacter*) and *Alphaproteobacteria* (*Rhodobacteraceae* and *Roseobacter*) as a result of a phytoplankton bloom (Alonso-Sáez et al., 2008; Wietz et al., 2021; Wilson et al., 2017; Zeng et al., 2013). On the contrary, *Thaumarchaeota* (*Nitrosopumilus maritimus*) and *Chloroflexi* (SAR202 clade), among others, were relatively low in summer, but dominant in winter communities (Alonso-Sáez et al., 2012; Grzymski et al., 2012; Müller et al., 2018; Wilson et al., 2017). Since temperature and the quantity and quality of dissolved organic carbon compounds are major drivers of the bacterial and archaeal community, changes of the vegetative season may have significant effects on the diversity and structure of these communities and consequently the microbial food web.

This study describes the pelagic microbial communities during three Nansen Legacy expeditions that took place during the summers of 2018, 2019, and 2021, investigating the hypothesis that differences in phytoplankton bloom status or nutrient concentrations will affect the bacterial and archaeal community.

2. Materials & methods

2.1. Sampling and environmental parameters

Samples were taken during the RV “Kronprins Haakon” cruises 2018707 (from Aug. 6th to 23rd 2018), 2019706 (from Aug. 5th to 27th 2019), and 2021708 (from July 12th to 29th 2021) along a transect in the Barents Sea east of Svalbard (Fig. 1). During the transect in 2018, only the first 5 stations, P1-P5 were sampled, while the transects of 2019 and 2021 included stations P6 and P7. Samples were taken using a Niskin rosette sampler following the Nansen Legacy protocol (The Nansen Legacy, 2021). Water samples were collected from the surface (5–10 m), the chlorophyll maximum, or if no clear maximum was found 20 m, 200 m, and deep (10–15 m above sea bottom; SUP 1). Samples from < 75 m were then defined as surface samples, based on the similarity of the bacterial and archaeal community of surface and deep samples. For all water samples 7 L of seawater were filtered on Sterivex filters (Merck, Darmstadt, Germany) and frozen immediately and kept at −80 °C until DNA extraction. During the cruises temperature, salinity, and the concentrations of phosphate, silicate, nitrate, and nitrite were measured (Chierici, 2021a, 2021b; Jones et al., 2022). In addition, seawater was filtered through GFF filters using vacuum filtration, and chlorophyll *a* was extracted for 12–24 h at 4 °C in the dark from algae collected on the filters using 5 ml methanol. The Chl a concentration was measured using a Turner design fluorometer. The abundance of phytoplankton cells was acquired on all cruises (Assmy et al., 2022a, 2022b, 2022c; Kohlbach et al., 2023). The bacterial and archaeal cell concentrations were determined using flow cytometry (The Nansen Legacy, 2021). Triplicates of 1.8 ml glutaraldehyde fixed seawater were used for flow cytometry using a FACS Calibur (Becton Dickinson, Oxford, UK) flow cytometer according to Marie and co-workers (Marie et al., 1999). Stained samples were counted at a low flow rate of around 60 μL min^{-1} and different groups of bacteria and archaea discriminated on a biparametric plot of green florescence (530/30) vs. side scatter (SSC,488/10).

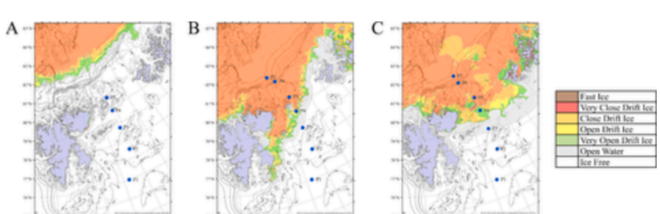

Fig. 1. Map of the Nansen Legacy transect in the Barents Sea with stations marked in blue and colour codes showing the ice conditions at the time of sampling in 2018 (A), 2019 (B), and 2021 (C). Ice data Credits: The Norwegian Ice Service - MET Norway. Ice data are from 15.08.2018, 15.08.2019, and 20.07.2021. Bathymetry Credits: NOAA National Centers for Environmental Information (NCEI); International Bathymetric Chart of the Arctic Ocean (IBCAO); General Bathymetric Chart of the Oceans (GEBCO).

2.2. DNA extraction and sequencing

The DNA of the samples was extracted using the DNeasy Power Water Sterivex Kit (QIAGEN, Hilden, Germany) according to the manual. From the extracted DNA sequencing libraries were prepared to target the V4 region of the 16S rRNA genes, using primers 515F – 5′-GTGYCAGCMGCCGCGGTAA-3′ and 806R – 5′- GGACTACNVGGGTWTCTAAT-3′ (Apprill et al., 2015; Parada et al., 2016). The libraries were sequenced using Illumina MiSeq technology with paired-end reads of 2 × 250 bp length at the Integrated Microbiome Resource in Halifax, Canada.

2.3. Sequence analyses

The raw sequences are available at the European Nucleotide Archive under the project number PRJEB57292. For the generation of Amplicon Sequence Variants (ASVs), the DADA2 pipeline was used in R (Callahan et al., 2016). Within the pipeline, primers were removed, the quality of the sequences checked, and a static trim with 250 bp and 220 bp was conducted. The resulting reads were dereplicated and used to generate ASVs. Subsequently, a merging step of the complementary reads was performed, chimeras removed, and the taxonomy of the ASVs assigned using a trained Silva database, based on the Silva release SSU Ref NR v138 (Quast et al., 2013). Thereafter, samples with < 10,000 sequences, and ASVs of mitochondria, chloroplasts, eukaryotes, and $< 1 \times 10^{-5}$ % of relative abundance were removed. Using the remaining reads, an approximate Maximum Likelihood tree was calculated using FastTree2 (Price et al., 2010) based on sequence alignments using mafft aligner (Katoh et al., 2002). The samples were then analyzed using weighted Unifrac distances for PERMANOVAs and Redundancy analyses (RDA). Correlations of the most abundant taxa with environmental variables were tested using the Pearson correlation method. The analyses were done using R and the “vegan”, “tidyverse”, “phyloseq”, “ggplot2”, “forcats”, “patchwork”, “scales”, “microbiomeSeq”, and “ape” packages (Lin Pedersen, 2020; Mazerolle, 2020; McMurdie and Holmes, 2013; Oksanen et al., 2020; Paradis and Schliep, 2019; R core team, 2021; Ssekagiri et al., 2017; Wickham, 2020; Wickham et al., 2019; Wickham and Seidel, 2020).

3. Results

3.1. Environmental variables and cell numbers

Temperatures ranged from 5.7 °C in surface waters to 1.8 °C and were higher in 2018 than in the other years (SUP 1). On ice free stations, the temperature was higher at the surface and decreased with depth, while the ice covered stations P6 and P7 showed negative temperatures in the first 40–60 m,which increased towards 200 m, andthen decreased again with depth (SUP 1). Salinities ranged around 34.9 at stations P1, P6, and P7 and around 34.5 at the other stations (SUP 1). Generally, the salinity increased after the first 5–40 m, an effect that was strong in ice covered stations,as a signature of ice melt (SUP 1). Similarly, the PO_4 concentrations increased with depth, reaching ~ 0.8 – 1.0 µmol l^{-1} for the deepest samples (SUP 1). The NO_2 concentrations were low ranging between 0.01 and 0.35 µmol l^{-1}, while NO_3 concentration were low in surface waters, but increased with depth (SUP 1). The SiO_4 concentrations also increased with depth ranging from > 0.7 µmol l^{-1} in surface waters up to 13.1 µmol l^{-1} (P7, 2021) at depth (SUP 1). Bacterial and archaeal cell abundance decreased from the surface to depth (SUP 1). Overall, cell numbers were lowest in 2018 and varied between stations in 2019 and 2021. At P2 - P5, and P7, cell numbers were higher in 2019, as compared to 2021, and showed the highest overall numbers at P5 with 2.3×10^6 cells ml^{-1} (SUP 1). While most stations showed distinct maxima in 2019, in 2021 maxima were only found at station P1 (8.7×10^5 cells ml^{-1}) and P6 (1.2×10^6 cells ml^{-1}; SUP 1).

Chl a concentrations were low in 2018, never exceeding 0.5 µg l^{-1}. In 2019, the Chl a concentrations were higher and distinct chlorophyll maxima were present at all stations (SUP 1). The highest Chl a concentrations were measured in 2021 (6.2 µg l^{-1} at P5) except P7 (Table 1; SUP 1). However, the highest integrated abundance of phytoplankton was found in 2019, where all stations exceeded 1×10^{10} cells per m^{-3}, with a maximum of 8.8×10^{10} cells per m^{-3} at station P6 (Table 1; Assmy et al., 2022b; Kohlbach et al., 2023). The phytoplankton was dominated by flagellates in 2019, especially *Heterosigma sp.* at stations P5 - P7 (Table 1; Kohlbach et al., 2023). The abundance was lower in 2021 with a maximum of 4.5×10^{10} cells per m^{-3} at P1 (Table 1; Assmy et al., 2022c). This peak was constituted by *Dinobryon* spp. Cells, while stations P4-P6 showed more diatom abundance and a peak of *Strombidium* sp. ciliates at P6 (Table 1; Kohlbach et al., 2023). Phytoplankton abundance was lowest in 2018, where only station P5 exceeded an abundance of 1.0×10^{10} cells per m^{-3} dominated by *Chysochromutina sp.* (Table 1; Assmy et al., 2022a; Kohlbach et al., 2023). In 2018 all stations were ice free, while in 2019 and 2021 stations P5 to P7 were covered with ice (Table 1). Station P4 was mostly ice covered in 2019 and station P3 and P4 became ice free just before sampling in 2021 (Table 1). Stations P1 and P2, as well as station P3 in 2018 and 2019, were ice free for at least a month before sampling (Table 1.

Table 1
Table with ice coverage, ice free time, maximum Chl a concentration and integrated phytoplankton cell abundance over the first 90 m (* first 30 m, # first 60 m) per station per year (Assmy et al., 2022a, 2022c, 2022b; Kohlbach et al., 2023; Assmy pers. comm.).

Year	Station	Ice cover [%]	Ice free time [days]	Chl a conc. maximum [µg l^{-1}]	Integrated phytoplankton abundance [cells m^{-3}]
	P1	0	220	0.42	5.1×10^9
	P2	0	86	0.38	6.0×10^9
2018	P3	0	80	0.26	1.7×10^9
	P4	0	76	0.06	9.6×10^8
	P5	0	76	0.24	1.2×10^{10}
	P1	0	89	1.22	2.9×10^{10}
	P2	0	43	1.24	3.3×10^{10} #
	P3	0	44	0.80	2.6×10^{10}
2019	P4	82	0	1.37	3.0×10^{10} *
	P5	95	0	2.57	6.9×10^{10}
	P6	93	0	1.29	8.8×10^{10}
	P7	95	0	1.74	1.8×10^{10}
	P1	0	195	3.49	4.5×10^{10}
	P2	0	39	2.17	9.8×10^9
	P3	0	1	1.53	3.5×10^9
2021	P4	0	2	6.08	1.0×10^{10}
	P5	98	0	6.19	1.4×10^{10}
	P6	93	0	2.72	1.4×10^{10}
	P7	100	0	0.23	4.6×10^9

* = Integrated over the first 30 m.
# = Integrated over the first 60 m.

3.2. Bacterial and archaeal community composition

The sequencing resulted in 11,713,482 unmerged input sequences and 4,301,652 merged sequences after all quality controls. PERMANOVA analyses of the bacterial and archaeal communities at all depths showed no significant differences between the samples, the stations, or the different years. The only significant differences was found between the surface and mesopelagic samples ($p = 0.007$; $n = 67$). Therefore, surface and deep samples were analysed separately. These analyses showed significant differences between 2018 and 2019/2021 in the surface ($p = 0.007$; $n = 29$), as well as at depth ($p = 0.035$; $n = 21$). Redundancy analyses (RDA) of the surface and mesopelagic waters showed significant correlations of the surface communities with temperature ($Pr(>F) = 0.046$), salinity ($Pr(>F) = 0.007$), and ice-free days ($Pr(>F) = 0.018$; Fig. 3). This separated most of the samples taken in 2018 and stations P1 and P2 from stations P3-P7 in 2019 and 2021. Significant correlations with the mesopelagic communities were found for station, depth, phosphate concentrations, cell abundance ($Pr(>F) < 0.01$), and salinity ($Pr(>F) = 0.038$; Fig. 2) thus separating stations P6 and P7 from stations P1 - P5.

The bacterial and archaeal community in all samples was dominated by *Alphaproteobacteria*, *Gammaproteobacteria*, *Bacteroidia*, and *Verrucomicrobia*, which made up > 99% of the surface community (Fig. 3). In the mesopelagic, these classes were still most abundant, but *Thermoplasmata*, members of the SAR324 clade, and specifically *Nitrosphaeria* increased to ~ 32% of the community, thus distinguishing deep samples from the surface water at all stations (Fig. 3).

During 2018, *Gammaproteobacteria* were most abundant with ~ 37% relative abundance at surface and depth, and maxima at stations P2 and P5, where relative abundances of 54.1% (P2; 180 m) and 44.6% (P5; 155 m) were found (Fig. 3). In 2019 and 2021 the relative abundance of *Gammaproteobacteria* was lower with total means of ~ 30% relative abundance (Fig. 4). Still, in 2021 at station P1 at 25 m, the highest *Gammaproteobacteria* abundance was found with 63.6% relative abundance (Fig. 3).

Among the *Gammaproteobacteria*, *Nitrincolaceae* were the most abundant with 18.6 ± 9.0%, 8.4 ± 6.2%, and 12.0 ± 10.8% in 2018, 2019, and 2021, where a maximum of 45.4% was reached (Fig. 4). *Pseudohongiella*, *Methylophagaceae*, and members of the SAR92, SAR86, and OM60(NOR5) clades were also found in higher relative abundance in surface waters as compared to deep waters throughout the sample set (Fig. 4). On the contrary, members of the SUP05 cluster were found in higher relative abundance at depth (Fig. 4).

Alphaproteobacteria were the second most abundant class in 2018 in surface waters with 33.0 ± 9.7% relative abundance in the surface and 21.1 ± 3.7% at depth (Fig. 3). In 2019 they constituted for 23.5 ± 14.7% total relative abundance and in 2021 with 21.0 ± 13.0% relative abundance in surface waters (Fig. 3). The *Alphaproteobacteria* were dominated by members of the SAR11 clade Ia with 19.3 ± 9.5% in 2018, 29.5 ± 17.6% in 2019, and 13.8 ± 10.7% in 2021 in the surface, decreasing to 11.6 ± 3.5%, 7.2 ± 4.6%, and 10.3 ± 6.0% in deep waters (Fig. 4). This was complemented by members of the SAT11 clade II, *Planktomarina*, and members of the SAR11 clade (Fig. 4).

The most distinct differences between surface and deep were found in the *Bacteroidia*, which showed a relative abundance of 27.4 ± 10.6%, 36.2 ± 20.5%, and 44.3 ± 19.7% at the surface in 2018, 2019, and 2021, as compared to 7.8 ± 2.8%, 8.9 ± 7.5%, and 7.2 ± 4.6% relative abundance at depth (Fig. 3). The high variations in surface water in 2019 resulted from abundances as high as 80.0% and 64.8% at stations P6 and P5 (Fig. 3). The relative abundance of different genera of *Bacteroidia* showed more variability with dominant genera being in high abundance at the surface of specific stations and generally in lower abundance at depth. *Polaribacter* was most abundant with 52.0% relative abundance at station P1 in 2021 and even 72.0% relative abundance at station P6 in 2019, dominated by the most abundant ASV in the dataset (57.3% relative abundance) (Fig. 4). *Cryomorphaceae* were found most

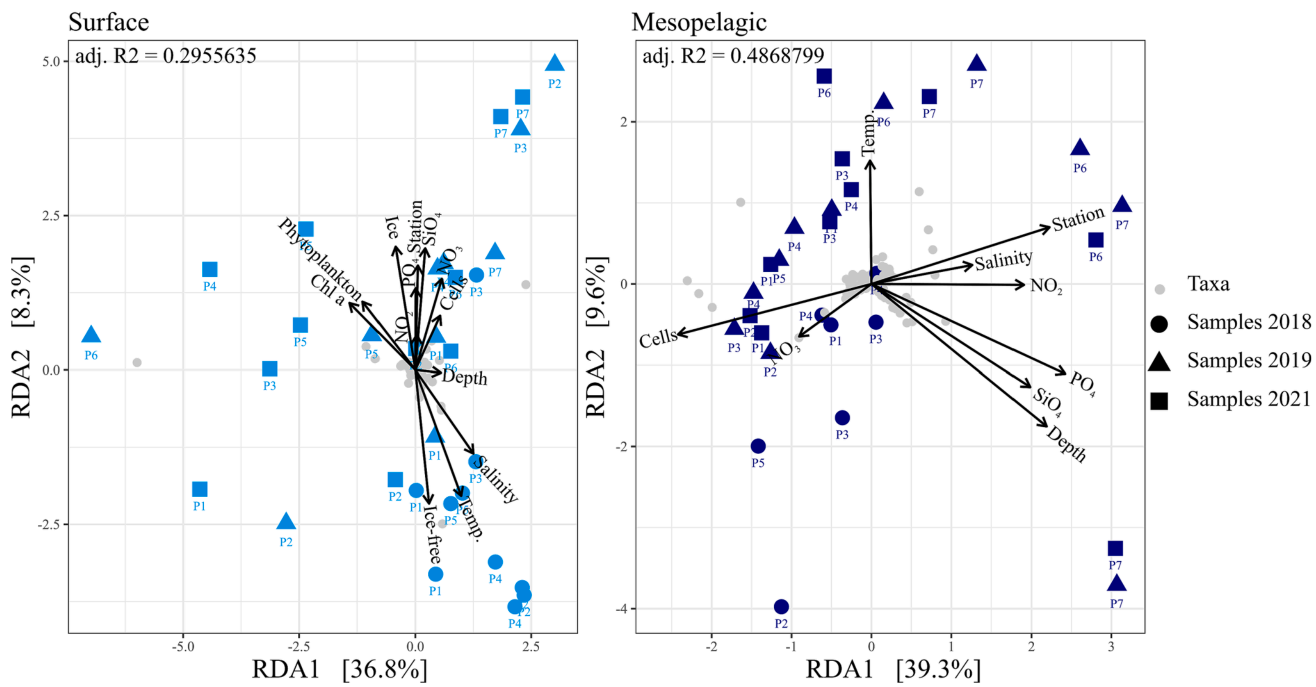

Fig. 2. Ordination plot of a redundancy analyses of all years separated by surface and mesopelagic. Environmental variables were abbreviated and units were omitted for readability (Ice = ice cover, Phytoplankton = Integrated phytoplankton cell abundance (90 m), Cells = Bacterial and archaeal cell abundance, Temp. = Temperature). Chl a concentration, Ice cover and ice free days were omitted in the RDA of the mesopelagic samples.

abundant at station P4 in 2018 and *Formosa* were highest at station P1 in 2019, both showing distinct fluctuations between stations in all years (Fig. 4). The fluctuations of the other dominant members, namely *Ulvibacter* and members of the NS5 clade, were not as distinct. Still *Ulvibacter* showed 13.8 ± 1.2% relative abundance in the surface waters of stations P4 and P5 in 2021 (Fig. 4).

Verrucomicrobia were the next abundant class in the surface ~ 2.5% relative abundance in all years, increasing to ~ 4.2% relative abundance at depth (Fig. 3). *Lentimonas* showed increased relative abundance in the surface waters, reaching a maximum of 12.0% in 2021 (Fig. 4). The archaeal *Nitrosphaeria* and *Thermoplasmata* were found in low relative abundance in the surface in all years, with the exceptions of three samples where they accounted for 2.1% and 0.2% at station P2 (2021), 11.5% and 1.7% at station P7 (2021), and 15.3% and 0.7% at station P3 (2019) (Fig. 3). At depth, these two groups were increased in all years with relative abundance up to 23.8 ± 3.3% (2019) and 7.8 ± 2.0% (2021; Fig. 3). *Cand.* Nitrosopumilus and members of the Marine Group II were the most abundant *Archaea* in deep waters with 8.8 ± 4.5% and 11.6 ± 4.5%, 20.1 ± 6.0% and 5.1 ± 2.6%, and 19.1 ± 6.8% and 6.5 ± 2.2% relative abundance in the consecutive years, both being nearly absent in surface waters of all years (Fig. 4). Similarly, members of the SAR324 clade and *Marinimicrobia* were almost exclusively found in deep waters with 4.1 ± 2.7%, 3.7 ± 2.4%, and 4.5 ± 2.3%, as well as 3.5 ± 2.5%, 3.1 ± 2.2%, and 3.5 ± 2.3% relative abundance in the different years (Fig. 4).

The most abundant taxa were used for correlation analyses with the environmental variables, resulting in a distinct pattern of "deep" taxa with the members of the SAR324 clade, the SAR11 clade II, the SUP05 cluster, Marine Group II archaea, *Cand.* Nitrosopumilus, and *Marinimicrobia* all correlated with depth and the correspondingly higher nutrient concentrations (Fig. 5). On the contrary, most taxa with higher relative abundance in the surface, such as *Polaribacter*, *Flavobacteriaceae*, *Ulvibacter*, *Cryomorphaceae*, *Nitrincolaceae*, the NS5 marine group, and SAR92 were negatively correlated to these variables, but positively correlated to Chl a (Fig. 5).

4. Discussion

The overall community structure, dominated by *Gammaproteobacteria*, *Alphaproteobacteria*, and *Bacteroidia* in the surface waters and by *Nitrosphaeria*, *Thermoplasmata*, *Marinimicrobia*, and members of the SAR324 clade in the deep waters, resemble previous reports of Arctic marine communities (de Sousa et al., 2019; Müller et al., 2018; Wilson et al., 2017). The distinct differences between the surface and the deep water communities were confirmed by Pearson correlations of the most abundant taxa, showing that surface taxa are positively correlated to Chl a and negatively correlated to nutrients and vice versa for deep taxa. Most *Bacteroidia* and *Gammaproteobacteria* show positive correlations with Chl a and negative correlations to nutrients and salinity, showing that Chl a, as compared to nutrients, is an important factor for the proliferation of the surface community. In deep waters, the nutrient concentrations and salinity are elevated and correlate with the most important taxa in these samples. The differences of communities in the deepest samples of stations P6 and especially P7 to other deep communities, are potentially due to the greater depth of > 500 m and the consequently higher abundance of "deep" taxa, such as *Marinimicrobia*, members of the SAR324 and SUP05 clades. The bottom depths of the other stations were between ~ 332 m (P4) and ~ 160 m (P5), potentially allowing for some mixing of the surface and the deep community, while this decreases with depth.

The high relative abundance of *Alphaproteobacteria*, consisting mainly of members of several SAR11 clades, is common for oligotrophic marine environments (Morris et al., 2002; Schattenhofer et al., 2009; Thiele et al., 2012; Wilson et al., 2017). On the contrary, the high relative abundance of *Gammaproteobacteria*, dominated by *Nitrincolaceae* (formerly *Oceanospirillaceae*) and *Bacteroidia*, dominated by *Polaribacter*, indicate waters with elevated concentrations of phytoplankton derived carbon sources (Gomez-Pereira et al., 2010; Puddu et al., 2003; Simon et al., 1999; Teeling et al., 2016, 2012; Thiele et al., 2012). *Nitrincolaceae* were found in Antarctic phytoplankton blooms and Arctic sea ice algal blooms, and are known for high diversity in carbon utilization metabolisms and rapid in response to increased carbon availability (Liu et al., 2020; Mönnich et al., 2020; Mori et al., 2019; Park

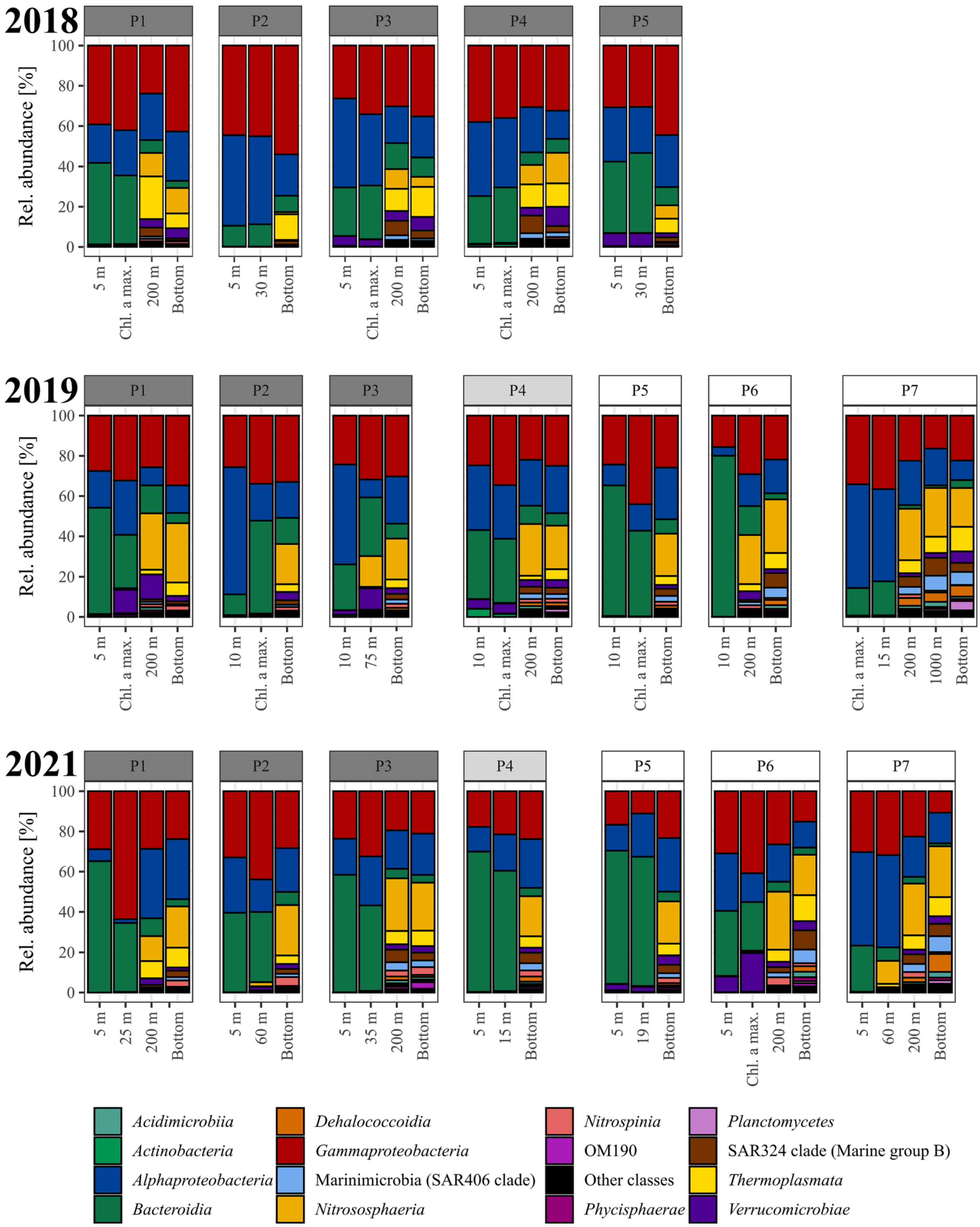

Fig. 3. Relative abundance of the 15 most abundant classes covering ~ 99% of all classes detected using 16S rRNA gene sequencing. The remaining classes are summed as "Other classes". Backgrounds of station names mark the ice coverage from open water (dark grey) to lose pack ice (grey) and dense pack ice (white) cover.

et al., 2020; Thiele et al., 2022). *Polaribacter* has frequently been found in correlation with phytoplankton blooms in polar, temperate, and tropical regions (Gomez-Pereira et al., 2010; Teeling et al., 2016; Thiele et al., 2015, 2012; Xing et al., 2015). These two taxa mark a prominent difference between the three years. While *Nitrincolaceae* are ~ 20 - 45% more abundant in 2018 surface waters, *Polaribacter* is ~70% more abundant in 2019 and ~ 80% more abundant in 2021 in the surface. As *Bacteroidia*, such as *Polaribacter*, *Lentimonas*, and *Ulvibacter*, have been found in high abundance in correlation with phytoplankton blooms due to their multitude of carbon degradation pathways and carbohydrate-active enzyme content (Gomez-Pereira et al., 2010; Reintjes et al., 2020, 2019; Teeling et al., 2016, 2012), this explains the correlation of the most abundant *Bacteroidia* with Chl a. These differences may point to an earlier postbloom stage of the community in 2019/2021 than in

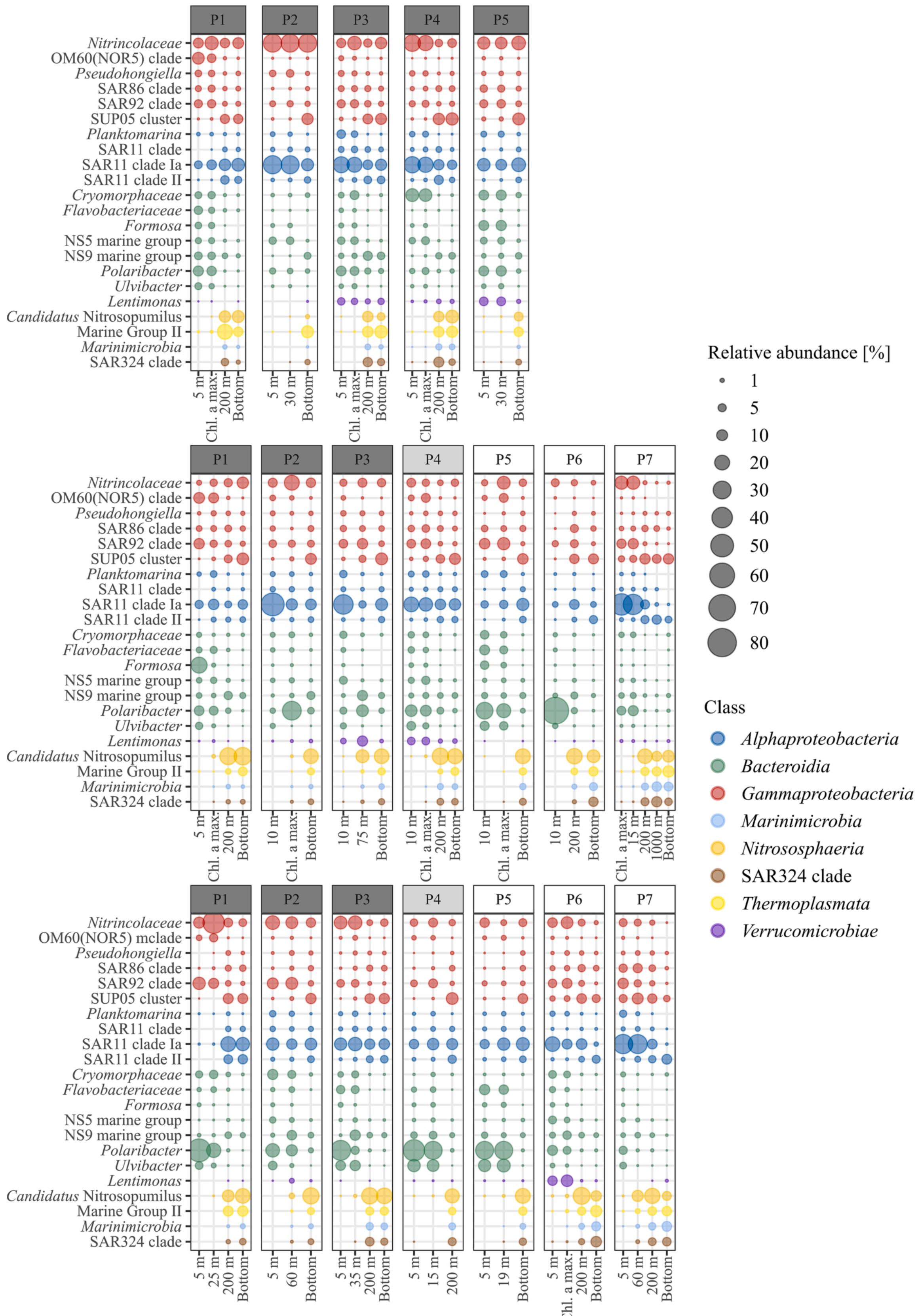

Fig. 4. Relative abundance of the most abundant taxa per class (color coded) for surface (●) and deep (■) waters of the stations P1 to P5 (2018) and P1 to P7 (2019/2021). Backgrounds of station names mark the ice coverage from open water (dark grey) to lose pack ice (grey) and dense pack ice (white) cover.

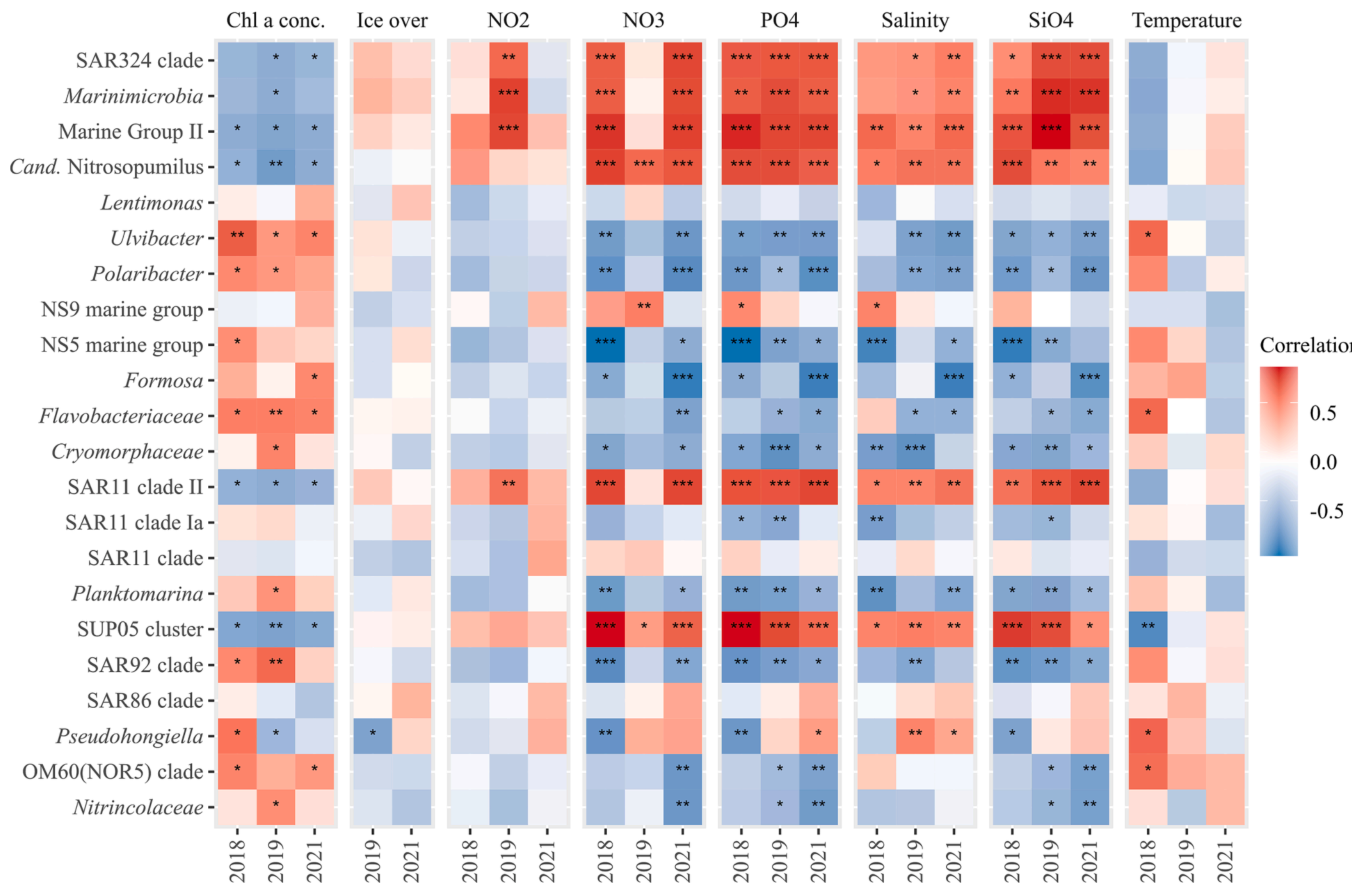

Fig. 5. Positive (red) and negative (blue) Pearson-correlations of the environmental variables and the most abundant taxa by year with significant correlations marked by * (* = p-value $\leq$ 0.05, ** = p-value $\leq$ 0.01, *** = p-value $\leq$ 0.001; p-values are Benjamini Hochberg adjusted).

2018. While samples in 2018 and 2019 were taken in August, samples of 2021 are from July, which could result in differences of the ecosystem state with respect to the state of the phytoplankton spring bloom. Therefore, we assume an earlier state of the bloom for 2021 than for 2019 and 2018. This is congruent with higher Chl a concentrations in 2021 than in the other years, potentially indicating the onset of a phytoplankton bloom. The lower Chl a concentrations, despite higher phytoplankton cell abundance in 2019 might indicate lower photosynthetic activity, thus indicating a later bloom stage. Similarly, Chl a concentrations and phytoplankton abundance are lower in 2018, indicating a late post bloom stage. These differences in the years could be aggravated by changes in the light environment and potentially earlier onset of the phytoplankton bloom due to differences in sea-ice cover (Dalpadado et al., 2020). This is supported by the significance of the ice free days, temperature, and salinity for the surface layer, where temperature and salinity were lower on ice covered stations, and in the separation of the samples from P1, P2, and all 2018 stations from samples from stations P3 - P7 in 2019/2021 in the RDA analyses. Lower temperatures and salinity are correlated to ice cover and might hence indirectly reflect the influence of ice cover on the bacterial and archaeal community. This influence is most likely a secondary effect. Sea ice cover reduces the light environment and hence leads to later onsets of phytoplankton blooms. These phytoplankton blooms then trigger a succession of the bacterial and archaeal community based on the availability of carbon sources. Therefore, the effect is secondary for the bacterial and archaeal community and direct correlations require larger investigations.

The bacterial and archaeal communities of stations P6 and P7 were distinctively different to the other stations sampled. The surface of station P7 was marked by the highest abundance of members of the SAR11 Clade in both years, thus indicating a rather oligotrophic state suggesting a pre-bloom or the onset of a phytoplankton bloom at these stations (Morris et al., 2002; West et al., 2008). Station P6 in 2019 was marked by an extreme dominance of *Polaribacter*, indicating the creation of favorable conditions for this taxon, potentially due to the ongoing *Heterosigma sp.* bloom. On the contrary, *Polaribacter* was relatively low on both stations in 2021. While Chl a values were low at P7, the Chl a concentrations were high at station P6. Here, the phytoplankton community was strongly dominated by *Strombidium* species (Kohlbach et al., 2023), which might not provide the preferred niche for *Polaribacter* or have exerted grazing pressure on the fast growing and hence larger *Polaribacter* cells, thus decimating their numbers (Chen et al., 2020).

The transport of Atlantic waters into the Arctic on the Svalbard Branch could potentially affect stations P1, P6, and P7 (Lind and Ingvaldsen, 2012; Loeng, 1991). In addition, the temperature profiles of stations P2 - P4 showed nearly opposite patterns than P6 and P7, which could be an indicator for different water bodies. However, a direct correlation of water bodies on the bacterial and archaeal community could not be proven and seems minor in the light of the "everything is everywhere" hypothesis (O'Malley, 2008). Secondary effects, like the drift of phytoplankton blooms and therefore carbon sources, towards these stations, may still affect the bacterial and archaeal community in the surface.

The dataset collected during three expeditions within the Nansen Legacy project showed differences of the bacterial and archaeal communities in surface waters of the Barents Sea based on the occurrence of phytoplankton and Chl a abundance, which can resemble different stages of the phytoplankton bloom and consequently carbon source availabilities. These community differences are mainly due to changes in the abundance of *Nitrincolaceae* and several *Bacteroidia* taxa, most prominently *Polaribacter*. The deep water communities were more stable and dominated by *Cand*. Nitrosopumilus, *Marinimicrobia*, and members of the SAR324 clade. Although indicating that higher average water temperatures, and less sea ice, could lead to earlier onsets of phytoplankton spring blooms, the consequences of these factors for the succession of the bacterial and archaeal community and the carbon dynamics within the microbial loop remain unclear. Over the short period of three summers, potential changes of the community dynamics might be masked by the high variability of the Arctic ecosystem. Hence, the long-term effects of global warming on the dynamics of the bacterial and archaeal communities, the microbial loop or the microbiology of the pelagic ecosystems of the Barents Sea require longer series of investigation.

Declaration of Competing Interest

The authors declare that they have no known competing financial interests or personal relationships that could have appeared to influence the work reported in this paper.

Data availability

Data will be made available on request.

Acknowledgement

This work was funded by the Research Council of Norway through the project The Nansen Legacy (RCN # 276730). We would like to thank the captain and crews of the RV Kronprins Haakon, as well as the leaders of the RF3 of The Nansen Legacy.

Appendix A. Supplementary data

Supplementary data to this article can be found online at https://doi.org/10.1016/j.pocean.2023.103054.

References

Alonso-Sáez, L., Sánchez, O., Gasol, J.M., Balagué, V., Pedrós-Alio, C., 2008. Winter-to-summer changes in the composition and single-cell activity of near-surface Arctic prokaryotes. Environ Microbiol 10, 2444–2454. https://doi.org/10.1111/j.1462-2920.2008.01674.x.

Alonso-Sáez, L., Waller, A.S., Mende, D.R., Bakker, K., Farnelid, H., Yager, P.L., Lovejoy, C., Tremblay, J.-É., Potvin, M., Heinrich, F., Estrada, M., Riemann, L., Bork, P., Pedrós-Alió, C., Bertilsson, S., 2012. Role for urea in nitrification by polar marine Archaea. Proc. Natl. Acad. Sci. U.S.A. 109, 17989–17994. https://doi.org/10.1073/pnas.1201914109.

Apprill, A., McNally, S., Parsons, R., Weber, L., 2015. Minor revision to V4 region SSU rRNA 806R gene primer greatly increases detection of SAR11 bacterioplankton. Aquat Microb Ecol 75, 129–137. https://doi.org/10.3354/ame01753.

Ardyna, M., Babin, M., Gosselin, M., Devred, E., Rainville, L., Tremblay, J.-É., 2014. Recent Arctic Ocean sea ice loss triggers novel fall phytoplankton blooms. Geophys Res Lett 41, 6207–6212. https://doi.org/10.1002/2014GL061047.

Arrigo, K.R., van Dijken, G.L., 2015. Continued increases in Arctic Ocean primary production. Prog Oceanogr. Synthesis of Arctic Research (SOAR) 136, 60–70. https://doi.org/10.1016/j.pocean.2015.05.002.

Årthun, M., Eldevik, T., Smedsrud, L.H., Skagseth, Ø., Ingvaldsen, R.B., 2012. Quantifying the Influence of Atlantic Heat on Barents Sea Ice Variability and Retreat. J. Climate 25, 4736–4743. https://doi.org/10.1175/JCLI-D-11-00466.1.

Assmy, P., Gradinger, R., Edvardsen, B., Wold, A., Goraguer, L., Wiktor, J., Tatarek, A., 2022a. Phytoplankton biodiversity Nansen Legacy JC1. https://doi.org/10.21334/NPOLAR.2022.C86F931F.

Assmy, P., Gradinger, R., Edvardsen, B., Wold, A., Goraguer, L., Wiktor, J., Tatarek, A., Dąbrowska, A.M., 2022b. Phytoplankton biodiversity Nansen Legacy Q3. https://doi.org/10.21334/NPOLAR.2022.DADCCF78.

Assmy, P., Gradinger, R., Edvardsen, B., Wold, A., Goraguer, L., Wiktor, J., Tatarek, A., Dabrowska, A.M., 2022c. Phytoplankton biodiversity Nansen Legacy JC2-1. https://doi.org/10.21334/NPOLAR.2022.AFE4302C.

Assmy, P., Fernández-Méndez, M., Duarte, P., Meyer, A., Randelhoff, A., Mundy, C.J., Olsen, L.M., Kauko, H.M., Bailey, A., Chierici, M., Cohen, L., Doulgeris, A.P., Ehn, J. K., Fransson, A., Gerland, S., Hop, H., Hudson, S.R., Hughes, N., Itkin, P., Johnsen, G., King, J.A., Koch, B.P., Koenig, Z., Kwasniewski, S., Laney, S.R., Nicolaus, M., Pavlov, A.K., Polashenski, C.M., Provost, C., Rösel, A., Sandbu, M., Spreen, G., Smedsrud, L.H., Sundfjord, A., Taskjelle, T., Tatarek, A., Wiktor, J., Wagner, P.M., Wold, A., Steen, H., Granskog, M.A., 2017. Leads in Arctic pack ice enable early phytoplankton blooms below snow-covered sea ice. Sci Rep 7, 40850. https://doi.org/10.1038/srep40850.

Callahan, B.J., McMurdie, P.J., Rosen, M.J., Han, A.W., Johnson, A.J.A., Holmes, S.P., 2016. DADA2: High-resolution sample inference from Illumina amplicon data. Nat Meth 13, 581–583. https://doi.org/10.1038/nmeth.3869.

Chen, W.-L., Chiang, K.-P., Tsai, S.-F., 2020. Neglect of Presence of Bacteria Leads to Inaccurate Growth Parameters of the Oligotrich Ciliate Strombidium sp. During Grazing Experiments on Nanoflagellates. Frontiers in Marine. Science 7.

Chierici, M., 2021a. Water column data on dissolved inorganic nutrients (nitrite, nitrate, phosphate and silicic acid) from the Nansen LEGACY seasonal cruise Q3, 2019706, with R.V. Kronprins Haakon, 5-27 August 2019. https://doi.org/10.21335/NMDC-1472517325.

Chierici, M., 2021b. Water column data on dissolved inorganic nutrients (nitrite, nitrate, phosphate and silicic acid) from the Nansen LEGACY joint cruise KH 2018707 with R.V. Kronprins Haakon, 8-20 August 2018. https://doi.org/10.21335/NMDC-839276558.

Dalpadado, P., Arrigo, K.R., van Dijken, G.L., Skjoldal, H.R., Bagøien, E., Dolgov, A.V., Prokopchuk, I.P., Sperfeld, E., 2020. Climate effects on temporal and spatial dynamics of phytoplankton and zooplankton in the Barents Sea. Prog Oceanogr 185, 102320. https://doi.org/10.1016/j.pocean.2020.102320.

de Sousa, A.G.G., Tomasino, M.P., Duarte, P., Fernández-Méndez, M., Assmy, P., Ribeiro, H., Surkont, J., Leite, R.B., Pereira-Leal, J.B., Torgo, L., Magalhães, C., 2019. Diversity and Composition of Pelagic Prokaryotic and Protist Communities in a Thin Arctic Sea-Ice Regime. Microb Ecol 78, 388–408. https://doi.org/10.1007/s00248-018-01314-2.

Gomez-Pereira, P.R., Fuchs, B.M., Alonso, C., Oliver, M.J., van Beusekom, J.E.E., Amann, R., 2010. Distinct flavobacterial communities in contrasting water masses of the North Atlantic Ocean. ISME J 4, 472–487.

Grzymski, J.J., Riesenfeld, C.S., Williams, T.J., Dussaq, A.M., Ducklow, H., Erickson, M., Cavicchioli, R., Murray, A.E., 2012. A metagenomic assessment of winter and summer bacterioplankton from Antarctica Peninsula coastal surface waters. ISME J 6, 1901–1915. https://doi.org/10.1038/ismej.2012.31.

Haug, T., Bogstad, B., Chierici, M., Gjøsæter, H., Hallfredsson, E.H., Høines, Å.S., Hoel, A. H., Ingvaldsen, R.B., Jørgensen, L.L., Knutsen, T., Loeng, H., Naustvoll, L.-J., Røttingen, I., Sunnanå, K., 2017. Future harvest of living resources in the Arctic Ocean north of the Nordic and Barents Seas: A review of possibilities and constraints. Fish Res 188, 38–57. https://doi.org/10.1016/j.fishres.2016.12.002.

Jones, E., Chierici, M., Hodal Lødemel, H., Møgster, J., Fonnes, L.L., 2022. Water column data on dissolved inorganic nutrients (nitrite, nitrate, phosphate and silicic acid) from Process (P) stations during the Nansen LEGACY joint cruise JC2-1, 2021708, with R.V. Kronprins Haakon, 14-24 July 2021. https://doi.org/10.21335/NMDC-1747434716.

Katoh, K., Misawa, K., Kuma, K., Miyata, T., 2002. MAFFT: a novel method for rapid multiple sequence alignment based on fast Fourier transform. Nucl Acids Res 30, 3059–3066. https://doi.org/10.1093/nar/gkf436.

Kohlbach, D., Bodur, Y., Müller, O., Amarant-Arumi, M., Blix, K., Bratbak, G., Chierici, M., Dabrowska, A.M., Dietrich, U., Gradinger, R., Hop, H., Jones, E., Martin Garcia, L., Olsen, L.M., Reigstad, M., Tatarek, A., Wiktor, J., Wold, A., Assmy, P., 2023. Low biomass summer season dominated by small phytoplankton and heterotrophic protists is likely to extend in a future Barents Sea with less sea ice. Progress in. Oceanography.

Li, W.K.W., McLaughlin, F.A., Lovejoy, C., Carmack, E.C., 2009. Smallest Algae Thrive As the Arctic Ocean Freshens. Science 326, 539. https://doi.org/10.1126/science.1179798.

Lin Pedersen, T., 2020. patchwork: The Composer of Plots. R package version 1 (1).

Lind, S., Ingvaldsen, R.B., 2012. Variability and impacts of Atlantic Water entering the Barents Sea from the north. Deep Sea Res. Part I 62, 70–88. https://doi.org/10.1016/j.dsr.2011.12.007.

Liu, Y., Blain, S., Crispi, O., Rembauville, M., Obernosterer, I., 2020. Seasonal dynamics of prokaryotes and their associations with diatoms in the Southern Ocean as revealed by an autonomous sampler. Environ Microbiol 22, 3968–3984. https://doi.org/10.1111/1462-2920.15184.

Loeng, H., 1991. Features of the physical oceanographic conditions of the Barents Sea. Polar Res 10, 5–18. https://doi.org/10.3402/polar.v10i1.6723.

Marie, D., Brussaard, C.P.D., Thyrhaug, R., Bratbak, G., Vaulot, D., 1999. Enumeration of Marine Viruses in Culture and Natural Samples by Flow Cytometry. Appl Environ Microbiol 65, 45–52.

Mazerolle, M.J., 2020. AICcmodavg: Model selection and multimodel inference based on (Q)AIC(c).

McMurdie, P.J., Holmes, S., 2013. phyloseq: An R Package for Reproducible Interactive Analysis and Graphics of Microbiome Census Data. PLoS One 8, e61217.

Mönnich, J., Tebben, J., Bergemann, J., Case, R., Wohlrab, S., Harder, T., 2020. Niche-based assembly of bacterial consortia on the diatom Thalassiosira rotula is stable and reproducible. ISME J 14, 1614–1625. https://doi.org/10.1038/s41396-020-0631-5.

Mori, J.F., Chen, L.-X., Jessen, G.L., Rudderham, S.B., McBeth, J.M., Lindsay, M.B.J., Slater, G.F., Banfield, J.F., Warren, L.A., 2019. Putative Mixotrophic Nitrifying-Denitrifying Gammaproteobacteria Implicated in Nitrogen Cycling Within the Ammonia/Oxygen Transition Zone of an Oil Sands Pit Lake. Front. Microbiol. 10 https://doi.org/10.3389/fmicb.2019.02435.

Morris, R.M., Rappe, M.S., Connon, S.A., Vergin, K.L., Siebold, W.A., Carlson, C.A., Giovannoni, S.J., 2002. SAR11 clade dominates ocean surface bacterioplankton communities. Nature 420, 806–810. https://doi.org/10.1038/nature01240.

Mueter, F.J., Broms, C., Drinkwater, K.F., Friedland, K.D., Hare, J.A., Hunt, G.L., Melle, W., Taylor, M., 2009. Ecosystem responses to recent oceanographic variability in high-latitude Northern Hemisphere ecosystems. Prog Oceanogr, Comparative

Marine Ecosystem Structure and Function: Descriptors and Characteristics 81, 93–110. https://doi.org/10.1016/j.pocean.2009.04.018.
Müller, O., Wilson, B., Paulsen, M.L., Rumińska, A., Armo, H.R., Bratbak, G., Øvreås, L., 2018. Spatiotemporal Dynamics of Ammonia-Oxidizing Thaumarchaeota in Distinct Arctic Water Masses. Front. Microbiol. 9 https://doi.org/10.3389/fmicb.2018.00024.
O'Malley, M.A., 2008. 'Everything is everywhere: but the environment selects': ubiquitous distribution and ecological determinism in microbial biogeography. Studies in History and Philosophy of Science Part C: Studies in History and Philosophy of Biological and Biomedical Sciences 39, 314–325. https://doi.org/10.1016/j.shpsc.2008.06.005.
Oksanen, J., Blanchet, F.G., Friendly, M., Kindt, R., Legendre, P., McGlinn, D., Minchin, P.R., O'Hara, R.B., Simpson, G.L., Solymos, P., Stevens, M.H.H., Szoecs, E., Wagner, H., 2020. vegan: Community Ecology Package. R package version 2.5-7.
Parada, A.E., Needham, D.M., Fuhrman, J.A., 2016. Every base matters: assessing small subunit rRNA primers for marine microbiomes with mock communities, time series and global field samples. Environ Microbiol 18, 1403–1414. https://doi.org/10.1111/1462-2920.13023.
Paradis, E., Schliep, K., 2019. ape 5.0: an environment for modern phylogenetics and evolutionary analyses in R. Bioinformatics 35, 526–528. https://doi.org/10.1093/bioinformatics/bty633.
Park, B.S., Lee, M., Shin, K., Baek, S.H., 2020. Response of the bacterioplankton composition to inorganic nutrient loading and phytoplankton in southern Korean coastal waters: A mesocosm study. Mar Ecol 41, e12591.
Polyakov, I.V., Pnyushkov, A.V., Alkire, M.B., Ashik, I.M., Baumann, T.M., Carmack, E. C., Goszczko, I., Guthrie, J., Ivanov, V.V., Kanzow, T., Krishfield, R., Kwok, R., Sundfjord, A., Morison, J., Rember, R., Yulin, A., 2017. Greater role for Atlantic inflows on sea-ice loss in the Eurasian Basin of the Arctic Ocean. Science 356, 285–291. https://doi.org/10.1126/science.aai8204.
Price, M.N., Dehal, P.S., Arkin, A.P., 2010. FastTree 2 – Approximately Maximum-Likelihood Trees for Large Alignments. PLoS One 5, e9490.
Puddu, A., Zoppini, A., Fazi, S., Rosati, M., Amalfitano, S., Magaletti, E., 2003. Bacterial uptake of DOM released from P-limited phytoplankton. FEMS Microbiol Ecol 46, 257–268. https://doi.org/10.1016/S0168-6496(03)00197-1.
Quast, C., Pruesse, E., Yilmaz, P., Gerken, J., Schweer, T., Yarza, P., Peplies, J., Glockner, F.O., 2013. The SILVA ribosomal RNA gene database project: improved data processing and web-based tools. Nucl Acids Res 41, D590–D596.
R core team, 2021. A language and environment for statistical computing. R Foundation for Statistical Computing, Vienna, Austria.
Rantanen, M., Karpechko, A.Y., Lipponen, A., Nordling, K., Hyvärinen, O., Ruosteenoja, K., Vihma, T., Laaksonen, A., 2022. The Arctic has warmed nearly four times faster than the globe since 1979. Commun Earth Environ 3, 1–10. https://doi.org/10.1038/s43247-022-00498-3.
Reigstad, M., Wassmann, P., Wexels Riser, C., Øygarden, S., Rey, F., 2002. Variations in hydrography, nutrients and chlorophyll a in the marginal ice-zone and the central Barents Sea. Journal of Marine Systems, Seasonal C-cycling variability in the open and ice-covered waters of the Barents Sea 38, 9–29. https://doi.org/10.1016/S0924-7963(02)00167-7.
Reintjes, G., Arnosti, C., Fuchs, B., Amann, R., 2019. Selfish, sharing and scavenging bacteria in the Atlantic Ocean: a biogeographical study of bacterial substrate utilisation. ISME J 13, 1119–1132. https://doi.org/10.1038/s41396-018-0326-3.
Reintjes, G., Fuchs, B.M., Scharfe, M., Wiltshire, K.H., Amann, R., Arnosti, C., 2020. Short-term changes in polysaccharide utilization mechanisms of marine bacterioplankton during a spring phytoplankton bloom. Environ Microbiol 22, 1884–1900. https://doi.org/10.1111/1462-2920.14971.
Sakshaug, E., 2004. Primary and Secondary Production in the Arctic Seas, in: Stein, R., MacDonald, R.W. (Eds.), The Organic Carbon Cycle in the Arctic Ocean. Springer, Berlin, Heidelberg, pp. 57–81. https://doi.org/10.1007/978-3-642-18912-8_3.
Schattenhofer, M., Fuchs, B.M., Amann, R., Zubkov, M.V., Tarran, G.A., Pernthaler, J., 2009. Latitudinal distribution of prokaryotic picoplankton populations in the Atlantic Ocean. Environ Microbiol 11, 2078–2093. https://doi.org/10.1111/j.1462-2920.2009.01929.x.
Simon, M., Glöckner, F., Amann, R., 1999. Different community structure and temperature optima of heterotrophic picoplankton in various regions of the Southern Ocean. Aquat. Microb. Ecol. 18, 275–284. https://doi.org/10.3354/ame018275.
Smedsrud, L.H., Esau, I., Ingvaldsen, R.B., Eldevik, T., Haugan, P.M., Li, C., Lien, V.S., Olsen, A., Omar, A.M., Otterå, O.H., Risebrobakken, B., Sandø, A.B., Semenov, V.A., Sorokina, S.A., 2013. The Role of the Barents Sea in the Arctic Climate System. Rev Geophys 51, 415–449. https://doi.org/10.1002/rog.20017.
Ssekagiri, A., Sloan, W., Ijaz, U., 2017. microbiomeSeq: An R package for analysis of microbial communities in an environmental context. https://doi.org/10.13140/RG.2.2.17108.71047.
Teeling, H., Fuchs, B., Becher, D., Klockow, C., Gardebrecht, A., Bennke, C.M., Kassabgy, M., Huang, S., Mann, A.J., Waldmann, J., Weber, M., Klindworth, A., Otto, A., Lange, J., Bernhardt, J., Reinsch, C., Hecker, M., Peplies, J., Bockelmann, F. D., Callies, U., Gerdts, G., Wichels, A., Wiltshire, K.H., Glöckner, F., Schweder, T., Amann, R.I., 2012. Substrate-controlled succession of marine bacterioplankton populations induced by a phytoplankton bloom. Science 336, 608–611.
Teeling, H., Fuchs, B.M., Bennke, C.M., Krüger, K., Chafee, M., Kappelmann, L., Reintjes, G., Waldmann, J., Quast, C., Glöckner, F.O., Lucas, J., Wichels, A., Gerdts, G., Wiltshire, K.H., Amann, R.I., 2016. Recurring patterns in bacterioplankton dynamics during coastal spring algae blooms. Elife 5, e11888.
The Nansen Legacy, 2021. Sampling Protocols: The Nansen Legacy Report Series. https://doi.org/10.7557/nlrs.5793.
Thiele, S., Fuchs, B.M., Ramaiah, N., Amann, R., 2012. Microbial community response during the iron fertilization experiment LOHAFEX. Appl Environ Microbiol 78, 8803–8812.
Thiele, S., Fuchs, B.M., Amann, R., Iversen, M.H., 2015. Colonization in the Photic Zone and Subsequent Changes during Sinking Determine Bacterial Community Composition in Marine Snow. Appl Environ Microbiol 81, 1463–1471. https://doi.org/10.1128/AEM.02570-14.
Thiele, S., Storesund, J.E., Fernández-Méndez, M., Assmy, P., Øvreås, L., 2022. A Winter-to-Summer Transition of Bacterial and Archaeal Communities in Arctic Sea Ice. Microorganisms 10, 1618. https://doi.org/10.3390/microorganisms10081618.
Wassmann, P., Duarte, C.M., Agustí, S., Sejr, M.K., 2011. Footprints of climate change in the Arctic marine ecosystem. Glob Chang Biol 17, 1235–1249. https://doi.org/10.1111/j.1365-2486.2010.02311.x.
West, N.J., Obernosterer, I., Zemb, O., Lebaron, P., 2008. Major differences of bacterial diversity and activity inside and outside of a natural iron-fertilized phytoplankton bloom in the Southern Ocean. Environ Microbiol 10, 738–756. https://doi.org/10.1111/j.1462-2920.2007.01497.x.
Wickham, H., 2020. forcats: Tools for Working with Categorical Variables (Factors). R package version (5).
Wickham, H., Averick, M., Bryan, J., Chang, W., McGowan, L.D., François, R., Grolemund, G., Hayes, A., Henry, L., Hester, J., Kuhn, M., Pedersen, T.L., Miller, E., Bache, S.M., Müller, K., Ooms, J., Robinson, D., Seidel, D.P., Spinu, V., Takahashi, K., Vaughan, D., Wilke, C., Woo, K., Yutani, H., 2019. Welcome to the Tidyverse. J Open Source Softw 4, 1686. https://doi.org/10.21105/joss.01686.
Wickham, H., Seidel, D., 2020. scales: Scale Functions for Visualization. R package version 1 (1), 1.
Wietz, M., Bienhold, C., Metfies, K., Torres-Valdés, S., von Appen, W.-J., Salter, I., Boetius, A., 2021. The polar night shift: seasonal dynamics and drivers of Arctic Ocean microbiomes revealed by autonomous sampling. ISME Commun 1, 1–12. https://doi.org/10.1038/s43705-021-00074-4.
Wilson, B., Müller, O., Nordmann, E.-L., Seuthe, L., Bratbak, G., Øvreås, L., 2017. Changes in Marine Prokaryote Composition with Season and Depth Over an Arctic Polar Year. Front. Mar. Sci. 4 https://doi.org/10.3389/fmars.2017.00095.
Xing, P., Hahnke, R.L., Unfried, F., Markert, S., Huang, S., Barbeyron, T., Harder, J., Becher, D., Schweder, T., Glöckner, F.O., Amann, R.I., Teeling, H., 2015. Niches of two polysaccharide-degrading Polaribacter isolates from the North Sea during a spring diatom bloom. ISME J 9, 1410–1422. https://doi.org/10.1038/ismej.2014.225.
Zeng, Y.-X., Zhang, F., He, J.-F., Lee, S.H., Qiao, Z.-Y., Yu, Y., Li, H.-R., 2013. Bacterioplankton community structure in the Arctic waters as revealed by pyrosequencing of 16S rRNA genes. Antonie Van Leeuwenhoek 103, 1309–1319. https://doi.org/10.1007/s10482-013-9912-6.